

# Preparation and electrochemical properties of nanofiber poly(2,5-dihydroxyaniline)/activated carbon composite electrode for supercapacitor

Lan Liu · Wei Wang · Wu-yuan Zou · Ben-lin He ·  
Ming-liang Sun · Min Wang · Xue-fei Xu

Received: 26 January 2010 / Revised: 7 March 2010 / Accepted: 11 March 2010 / Published online: 8 April 2010  
© Springer-Verlag 2010

**Abstract** In this study, poly(2,5-dihydroxyaniline) (PDHA) was successfully prepared by electrochemical method on the surface of active carbon (AC) electrodes. The physical and electrochemistry properties of PDHA/AC composite electrode compared with pure AC electrode were investigated by scanning electronic microscope (SEM), cyclic voltammetry (CV), electrochemical impedance spectroscopy, cycle life test. From SEM, PDHA presents nanofiber network morphology. The diameter of the nanofiber PDHA is about 200–300 nm. PDHA/AC composite electrode shows redox peaks in CV curve and voltage plateaus in galvanostatic charge–discharge curve, and all these indicate that PDHA/AC composite electrode has more advantages. The maintenance of the capacitance compared to initial cycle capacitance of composite electrode is about 90% during the charge–discharge cycles. In conclusion, The PDHA/AC composite electrode shows much higher specific capacitance ( $958 \text{ F g}^{-1}$ ), better power characteristics, longer cycle life. Therefore, PDHA/AC composite electrodes were more promising for application in capacitor. This can be attributed to the introduction of nanofiber PDHA. The effect and role of PDHA in the composite electrodes were also discussed in detail.

**Keywords** Supercapacitors · AC · PDHA · Capacitance

## Abbreviations

PDHA Poly(2,5-dihydroxyaniline)

AC	Active carbon
PDHA/AC	Poly(2,5-dihydroxyaniline)/activated carbon
SEM	Scanning electronic microscope
CV	Cyclic voltammetry
EIS	Electrochemical impedance spectroscopy
C	Carbon
PVDF	Polyvinylidene fluoride

## Introduction

With a growing demand for power sources, supercapacitors are attracting great interest because of higher specific power than batteries and higher specific energy than conventional capacitors [1–3]. Electrode material, as an important part of supercapacitors, has also drawn considerable attention; many researches have been focused on electrode material.

Three different types of supercapacitors are commonly described in literature [1], depending on the nature of the active material used: activated carbon [4–10], conducting polymer [11–16], and metal-oxide [17–19].

In electrochemical double-layer capacitor, porous activated carbon (AC) is utilized as the active electrode material due to its high porosity, good conductivity, low cost, and high surface area. However, in practice, the upper limit for the measured capacitance of activated carbon electrode is generally about  $200 \text{ F g}^{-1}$  in aqueous electrolytes [11].

Deposition with conducting polymers has been considered as one of the favorable methods for carbon modification [3, 20]. Conducting polymers such as polyaniline (PANI) [20–30], polypyrrole [31], polythiophene [32], and their derivatives have been recognized as the electrode materials for the supercapacitor application. Moreover, PANI and its derivatives show a lot of advantages for

L. Liu · W. Wang (✉) · W.-y. Zou · B.-l. He · M.-l. Sun ·  
M. Wang · X.-f. Xu  
Institute of Material Science and Engineering,  
Ocean University of China,  
Qingdao 266100, People's Republic of China  
e-mail: clwang@ouc.edu.cn

practical applications, such as ease of polymerization in aqueous media and good stability in air.

Recently, obvious progress has been made in designing and fabricating composites [23–28]. Among these studies, Bin Dong et al. [26] reported the polyaniline/multiwalled carbon nanotubes composite electrode synthesized by an in situ chemical oxidative polymerization method. Wei-Chih Chen et al [21] reported the electropolymerization of PANI on the surface of activated porous carbons.

However, to the best of our knowledge, no studies have been focused on the fabricating of poly(2,5-dihydroxyaniline) and activated carbon. Therefore, in this study, we first attempt to prepare PDHA/AC electrode. Finally, we have successfully prepared nanofiber network PDHA. The physical and electrochemical properties were characterized by SEM, EIS, galvanostatic charge–discharge test, and cycle life test.

## Experimental section

### Preparation of activated carbon electrodes

Weigh a certain amount of AC, C, and PVDF; add *N*-methyl pyrrolidone as dispersing agent; heat the mixture in the electromagnetic heating furnace; put the slurry on stainless steel mesh evenly (work area, 10×10 mm); while it is viscous, place electrodes in vacuum-drying oven.

### Preparation of PDHA/AC composite electrodes

Electrochemical measurements were carried out with a three-electrode configuration. Ag/AgCl (Shanghai Electrical Instrument Works) was used as the reference electrode, AC electrode (10×10 mm) as the working electrode, and platinum foil (10×10 mm) as the counter electrode. All potentials reported here were measured vs. Ag/AgCl. Poly(2,5-dimethoxyaniline) film was electrochemically loaded on the AC electrodes through cyclic voltammetry (CV) in a potential range between –0.2 and 0.8 V with the scan rate of 5 mV s<sup>–1</sup> in the solution containing 0.5 mol L<sup>–1</sup> H<sub>2</sub>SO<sub>4</sub> and 0.2 mol L<sup>–1</sup> 2,5-dimethoxyaniline; Then, poly(2,5-dimethoxyaniline)/AC electrode was used as the working electrode, poly(2,5-dihydroxyaniline) was obtained through hydrolysis reaction on poly(2,5-dimethoxyaniline)/AC electrode by CV in a potential range between –0.2 and 0.8 V with the scan rate of 5 mV s<sup>–1</sup> in the solution containing 0.5 mol L<sup>–1</sup> H<sub>2</sub>SO<sub>4</sub>.

### Measurements

CV and surface morphology of the resulting electrodes were characterized, respectively, using an electrochemical work-

station LK9805Z (Lanlike Company, Tianjin) and a SEM (JSM-6700F, Japan). The Impedance Spectrum Analyzer, IM6 (ZAHNER, Germany), with Thales software was employed to measure the ac impedance spectra of electrodes at applied Potential of 0.4 V. The potential amplitude of ac was kept as 5 mV, and a wide frequency range of 10 mHz–100 kHz was used. The charge–discharge behavior of electrodes and cycle life were examined by chronopotentiometry using LAND CT2001A (Jinnuo Company, Wuhan).

## Results and discussion

### Morphology analysis

The morphologies of electrodes play an important role on the performances of electrodes. SEM picture of PDHA was shown in Fig. 1. The film presents nanofiber network

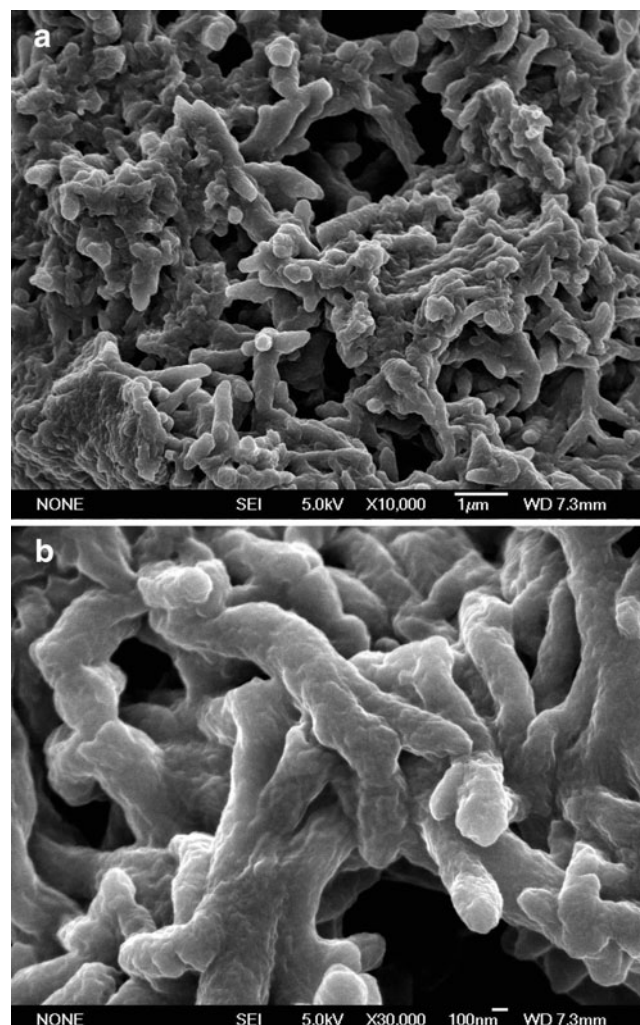


**Fig. 1** SEM photos of the PDHA/AC electrode: (magnification **a** ×10,000 **b** ×30,000)

porous morphology. The diameter of the nanofiber PDHA is about 200–300 nm. In general, nanofiber PDHA intertwined together to form a three-dimensional reticulation, which may cause remarkable rising of conductive pathway and lead to high conductivity, and the network nanofiber and porous morphology may enable effective and rapid access of the electrolyte and storage in three dimensions, which results in high charge storage and fast charge–discharge processes. In conclusion, this kind of composite electrodes exhibit both desired faraday pseudo capacitance and considerable double-layer capacitance. Therefore, it will be an ideal candidate as electrode material for supercapacitors.

#### Cyclic voltammetry test

Figure 2 gives CV curves of AC and PDHA/AC composite electrodes in the potential range of  $-0.2$  to  $0.8$  V at the scan rate of  $1$  mV/s in  $0.5$  mol/L  $H_2SO_4$  solution. As was shown in Fig. 2, CV curve of AC electrode shows rectangular-like feature that is a typical  $I$ – $E$  response of AC electrode in aqueous media, revealing double-layer charge–discharge characteristic. This is in agreement with results reported in the literature [7, 21, 25, 27]. For PDHA/AC composite electrode, the current significantly increases for the potential beyond  $0.2$  V and decreases below  $0.6$  V during the anodic potential sweep. This is resulted from faradaic current of conducting state PDHA in the potential of  $0.2$  to  $0.6$  V. On the other hand, while the potential is below  $0.2$  V, PDHA exists in the insulating state that could not generate faradaic current. The current is enhanced due to the reduction of PDHA in the reversal cathodic potential sweep. In addition, the peak-to-peak potential separation between the oxidation and reduction peaks is so small

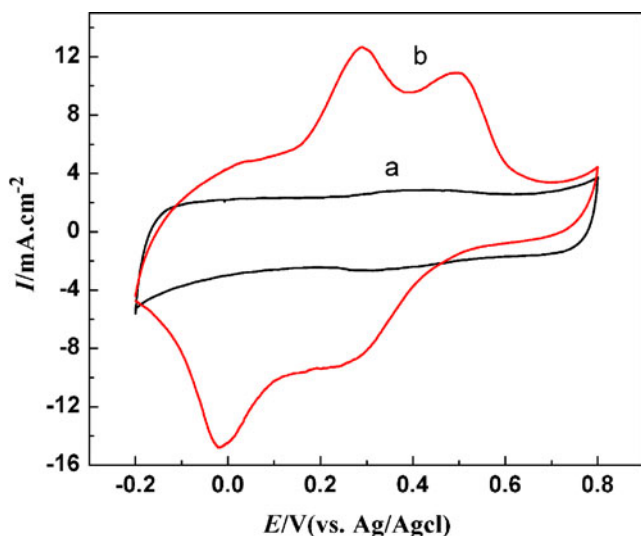


**Fig. 2** Cyclic voltammograms of the AC (a) and PDHA/AC (b) electrodes at the scan rate of  $1$  mV/s

which indicates that the PDHA/AC composite electrode shows good reversibility.

Moreover, from a comparison of all curves in Fig. 2, larger voltammetric output currents occur at the PDHA/AC composite electrode than the pure AC electrode. Since capacitance can be estimated from the output current divided by the scan rate [26], this implies that the capacitance of the composite is larger than that of the pure AC electrode. We can draw a conclusion that PDHA/AC composite electrode has considerable faraday pseudo-capacitance and double-layer capacitance. This conclusion is further improving that this kind of high specific area nanofiber porous PDHA allow excellent electrolyte access and storage in three dimensions, resulting in high charge storage and fast charge–discharge processes. However, accurate capacitance values should be obtained from the galvanostatic charge–discharge experiments.

#### Galvanostatic charge-discharge test

The charge–discharge behavior of AC and PDHA/AC composite electrodes were examined by chronopotentiometry, and typical results measured from  $0$  to  $0.8$  V in  $0.5$  mol/L  $H_2SO_4$  solution at  $3$  mA  $cm^{-2}$  are shown in Fig. 3.

For AC electrode, potential–time curve shows linear relationship indicating the slope of galvanostatic charge–discharge curve is essentially constant, showing double-layer characteristic [7, 29]. This conclusion is consistent with the result of CV analysis.

Compared to AC electrode, it could be seen that the curve of PDHA/AC composite electrode is not ideal straight line, indicating the process of faradic reaction. Longer charge/discharge duration is shown due to the combination of electric double-layer capacitance and

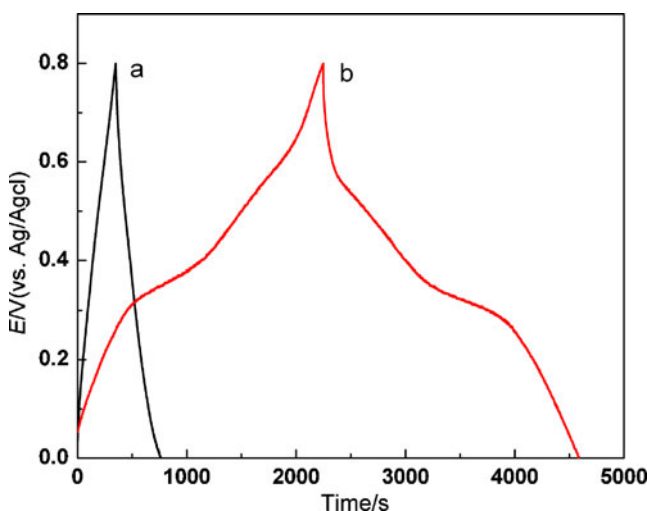


**Fig. 3** Galvanostatic charge-discharge curves of AC (a) and PDHA/AC (b) electrodes at current density of  $3$  mA  $cm^{-2}$

faradaic capacitance. Moreover, it can be obviously found that there are voltage plateaus between 0.2 and 0.5 V in charge–discharge process, respectively. The voltage plateaus correspond to redox reactions of PDHA, which is also consistent with the result of CV test. In addition, note that all the charge curves are very symmetric to their corresponding discharge counterparts in the whole potential region of investigation, which indicate that a reversible oxidation occurs among the electrode materials.

The discharge average specific capacitance of these electrodes can be obtained from these discharge curves according to the following equation [26].

$$C = \frac{I \times t}{\Delta V \times m} \quad (1)$$

Where  $C$  is specific capacitance,  $I$  is discharge current,  $t$  is the discharge time,  $\Delta V$  is average discharge potential, and  $m$  is the mass of active material within the electrode.

In accordance with Eq. 1, Table 1 summarized the specific discharge capacitance of AC and PDHA/AC electrodes as a function of discharge current density. It can be seen that PDHA/AC composite electrodes have consistent higher specific capacitance than pure AC electrode, although the specific capacitance of pure AC and PDHA/AC composite electrodes all decrease gradually with the increasing discharge current density. At current density of  $3 \text{ mA cm}^{-2}$ , the PDHA/AC composite electrode shows a higher specific capacitance of  $958 \text{ F g}^{-1}$ . Moreover, compared with pure AC electrode, the capacitance-decreasing rate with increasing discharge current density for PDHA/AC electrodes is lower. At a current density of  $15 \text{ mA cm}^{-2}$ , the specific capacitance of PDHA/AC electrodes is still as high as  $740 \text{ F g}^{-1}$ , which is about 77% of the specific capacitance at current density of  $3 \text{ mA cm}^{-2}$ . The capacitance maintenance of pure AC electrode is about 64%. This indicates that PDHA/AC composite electrode have better power characteristics than pure AC electrode. The reason may be: the addition of PDHA to AC makes the composites with interwoven fibrous network structure, which improves the conductivity and facilitates access of the electrolyte, and makes decrease of the specific capacitance is more slowly even at high discharge current density.

**Table 1** Specific capacitance of AC and PDHA/AC electrodes at different current densities

Current density [ $\text{mA cm}^{-2}$ ]	3	5	15
Specific capacitance of AC electrode [ $\text{F g}^{-1}$ ]	336	264	215
Specific capacitance of PDHA/AC electrode [ $\text{F g}^{-1}$ ]	958	748	740

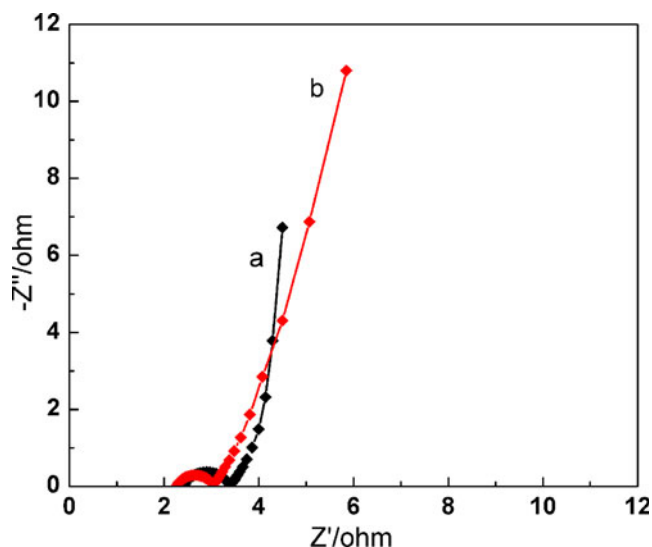


**Fig. 4** Impedance spectra of AC (a) and PDHA/AC (b) electrodes at applied voltage of 0.4 V

#### Impedance spectra test

The electrochemical impedance spectra are used to study mechanistic aspects further. From the redox peaks voltage of CV test and voltage plateaus of galvanostatic charge–discharge curves, we infer that the conductance of PDHA is minimum at approximately 0.4 V. Therefore, typical Nyquist diagrams for the AC and PDHA/AC electrodes in  $0.5 \text{ mol L}^{-1} \text{ H}_2\text{SO}_4$  solution at applied potential of 0.4 V were shown in Fig. 4.

Note that all the impedance spectra show a single semicircle in the high-frequency region and a sloped line which is indicative of a redox layer produced by the ac stimulation penetrating the entire depth of the polymer film

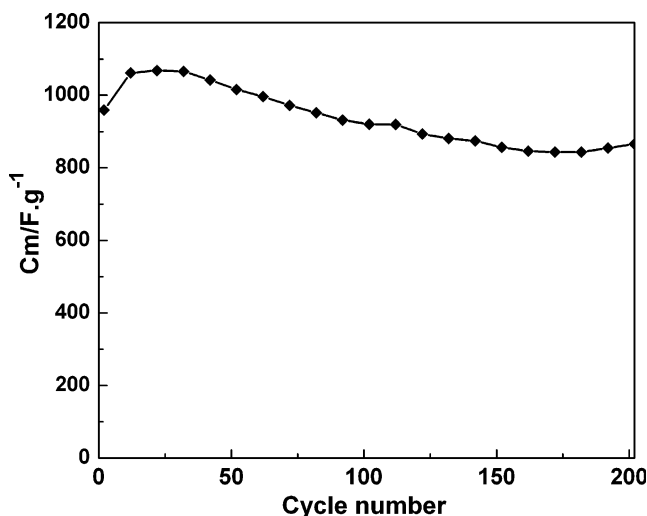


**Fig. 5** Cycle life of PDHA/AC electrode



in the low-frequency region [33]. The linear part with 45° slope appearing in a transitory way next to the semicircle indicates the diffusion limitation in the doping–undoping process. From the point intersecting with the real axis in the region of high frequency, internal resistance can be obtained, which is related to several reasons: the ionic resistance of the electrolyte, the intrinsic resistance of active material, and the contact resistance at the interface active material [26, 34]. The semicircle diameter implies the charge transfer resistance [35]. Internal resistances of pure AC and PDHA/AC composite electrodes are almost the same. However, it is clearly seen that PDHA/AC composite electrode includes a semicircle with smaller diameter than pure AC, indicating its lower charge-transfer impedance. It is further proven that porous nanofiber PDHA coated on AC electrode may have excellent active sites and conductivity, which makes ion intercalation distance to a matter of nanometer and facilitates the charge transfer and reduces internal resistance. Further demonstrating PDHA/AC composite electrodes have better power characteristics and were more promising for application in capacitor than pure AC electrodes.

#### Cycle life test

Since degradation of conducting polymers is usually found when they are potential cycled in aqueous media [29], cycle life is very important to the electrode material, so the stability of PDHA/AC electrode has to be examined in order to evaluate their practical applicability. Typical galvanostatic charge-discharge cycling results of PDHA/AC electrode at current densities of 3 mA cm<sup>-2</sup> in the potential ranges of 0.0 to 0.8 V for 200 cycles were employed to investigate the cyclic life. In addition, Fig. 5 showed the specific discharge-specific capacitance of the PDHA/AC electrode as a function of cycle numbers. During the initial cycle, capacitance of 958 F g<sup>-1</sup> is obtained. There is a gradual increase up to 1,068 F g<sup>-1</sup> in about 30 cycles, the reason may be the activation process of PDHA, and then it remains fairly constant up to 200 charge–discharge cycles. The maintenance of the capacitance of composite electrode is about 90% during the charge–discharge cycles (compared with capacitance of initial cycle). The capacitance decay is probably due to the degradation of PDHA during cycling. Swelling and deswelling of this electroactive polymer may also lead to degradation. Thus, PDHA deposited on activated carbon is fairly adherent and stable and retains its electrochemical capacitance property over a large number of cycles. The result is consistent with that indicated above. Therefore, we can draw a conclusion: this kind of composites can be considered as promising materials in the application of supercapacitors.

#### Conclusion

In summary, nanofiber network PDHA was prepared successfully through electrochemical method. High value of capacitance up to 958 F g<sup>-1</sup> of the PDHA/AC has been obtained at current density of 3 mA cm<sup>-2</sup>, which is better than the reports value of PANI/AC electrodes [21, 25]. The results indicate that this kind of PDHA has more active sites, excellent conductivity, which result in high charge-storage and fast charge-discharge processes and smaller internal resistance. So the PDHA/AC composites proposed here will be effectively used as electrodes

**Acknowledgements** We would like to thank the National Natural Science Foundation of China (Grant No. 50642011) and the Natural Science Foundation of Shandong Province of China (Grant No. 2006GG2207006) for the financial support.

#### References

1. Conway BE (1991) *J Electrochem Soc* 138:1539–1548
2. Arbizzani C, Mastragostino M, Soavi F (2001) *J Power Sources* 100:164–170
3. Kotz R, Carlen M (2000) *Electrochim Acta* 45:2483–2498
4. Gamby J, Taberna PL, Simon P, Fauvarque JF, Chesneau M (2001) *J Power Sources* 101:109–116
5. Ruiz V, Blanco C, Santamaria R, Ramos-Fernández JM, Martínez-Escandell M, Sepúlveda-Escribano A, Rodríguez-Reinoso F (2009) *Carbon* 47:195–200
6. Chen QL, Xue KH, Shen W, Tao FF, Yin SY, Xu W (2004) *Electrochim Acta* 49:4157–4161
7. Seo MK, Park SJ (2009) *Mater Sci Eng B* 164:106–111
8. Qu DY (2002) *J Power Sources* 109:403–411
9. Taberna PL, Chevallier G, Simon P, Plée D, Aubert T (2006) *Mater Res Bull* 41:478–484
10. Momma T, Liu XJ, Osaka T, Ushio Y, Sawada Y (1996) *J Power Sources* 60:249–253
11. Snook GA, Wilson GJ, Pandolfo AG (2009) *J Power Sources* 186:216–223
12. Conway BE, Pell WG (2003) *J Solid State Electrochem* 7:637
13. Kalaji M, Murphy PJ, Williams GO (1999) *Synth Met* 102:1360–1361
14. Mastragostino M, Arbizzani C, Soavi F (2001) *J Power sources* 97–98:812–815
15. Mastragostino M, Arbizzani C, Soavi F (2002) *Solid State Ionics* 148:493–498
16. Inzelt G (2008) *Conducting polymers*. Springer, Heidelberg
17. Subramanian V, Hall SC, Smith PH, Rambabu B (2004) *Solid State Ionics* 175:511–515
18. Prasad KR, Miura N (2004) *Electrochem Commun* 6:849–852
19. Prasad KR, Miura N (2004) *Electrochem Commun* 6:1004–1008
20. Lin YR, Teng H (2003) *Carbon* 41:2865–2871
21. Chen WC, Wen TC (2003) *J Power Sources* 117:273–282
22. Zhou HH, Chen H, Luo SL, Lu GW, Wei WZ, Kuang YF (2005) *J Solid State Electrochem* 9:574–580
23. Sivakkumar SR, Kim WJ, Choi JA, MacFarlane DR, Forsyth M, Kim DW (2007) *J Power Sources* 171:1062–1068
24. Mondal SK, Barai K, Munichandraiah N (2007) *Electrochim Acta* 52:3258–3264
25. Wang Q, Li JL, Gao F, Li WS, Wu KZ, Wang XD (2008) *New Carbon Materials* 3:275–280

26. Dong B, He BL, Xu CL, Li HL (2007) *Mater Sci Eng B* 143:7–13
27. Bleda-Martínez MJ, Morallón E, Cazorla-Amorós D (2007) *Electrochim Acta* 52:4962–4968
28. He BL, Dong B, Wang W, Li HL (2009) *Mater Chem Phys* 114:371–375
29. Hu CC, Li WY, Lin JY (2004) *J Power Sources* 137:152–157
30. Xu GC, Wang W, Qu XF, Yin YS, Chu L, He BL, Wu HK, Fang JR, Bao YS, Liang L (2009) *Eur Polym J* 45:2701–2707
31. Muthulakshmi B, Kalpana D, Pitchumani S, Renganathan NG (2006) *J Power Sources* 158:1533–1537
32. Laforgue A, Simon P, Sarrazin C, Fauvarque JF (1999) *J Power Sources* 80:142–148
33. Hong JI, Yeo IH, Paik WK (2001) *J Electrochem Soc* 148:156–164
34. Mi HY, Zhang XG, Yang SD, Ye XG, Luo JM (2008) *Mater Chem Phys* 112:127–131
35. Guo DJ, Li HL (2005) *J Solid State Electrochem* 9:445–449